Toxicology and Applied Pharmacology 511 (2026) 117804

Contents lists available at ScienceDirect

Toxicology and Applied Pharmacology

journal homepage: www.elsevier.com/locate/taap

Camizestrant-induced heart rate reduction is mediated via a sinoatrial node pacemaker channel mechanism

Andrew Hall [a], Saïd El-Haou [b], Inmaculada C. Villar [a], David Molla [c], Maggie Kwan [d], Stuart Purbrick [a], David Henry [e], Jason Kirk [e], Glen Hawthorne [a], Serena Canzolino [c], Joanna Harding [e,1], Alexander Harmer [a], Annalisa Bucchi [c], Liz Roberts [b], Amy Pointon [a], Stephanie Protze [d], Mirko Baruscotti [c], Lindsay Wright [a,*]

[a] Clinical Pharmacology and Safety Sciences, R&D, AstraZeneca, Cambridge, United Kingdom
[b] Discovery Sciences, R&D, AstraZeneca, Cambridge, United Kingdom
[c] Department of Biosciences, The Cell Physiology MiLab, Università degli Studi di Milano, Milan, Italy
[d] McEwen Stem Cell Institute, University Health Network, Toronto, Ontario, Canada
[e] Clinical Pharmacology and Safety Sciences, AstraZeneca, Cambridge, United Kingdom

ARTICLE INFO

Editor: Lawrence Lash

Keywords:
Selective Estrogen Receptor Degrader
Complete Estrogen Receptor Antagonist
Cardiac Effects
Pacemaker Current
Nonclinical Models

ABSTRACT

Camizestrant, a next-generation selective estrogen receptor (ER) degrader and complete ER antagonist, has been associated with a reversible dose- and time-dependent heart rate (HR) reduction in clinical studies. This nonclinical investigation aimed to understand the mechanism of camizestrant-induced HR reduction. The effects of camizestrant on HR in vivo were assessed in rat and dog telemetry studies. Effects on pacemaker channel function in vitro were assessed using patch-clamp electrophysiology in Chinese hamster ovary cells expressing human hyperpolarization-activated cyclic nucleotide-gated channel 4 (hHCN4), human embryonic stem cell (hESC)-derived sinoatrial node (SAN) cardiomyocytes, and primary rat SAN cardiomyocytes. In dogs, 28-day repeat-dose camizestrant administration caused a reversible dose- and time-dependent HR reduction (maximum reduction of 53 beats per min [bpm] on Day 25 vs pre-study levels at 20 mg/kg). HR reduction was also noted in rats (maximum reduction 89 bpm vs vehicle [23%] on Day 5 of a 7-day study at 75 mg/kg). Responses to chronotropic stimuli (e.g., atropine and isoprenaline) were reduced in dogs treated with camizestrant. Camizestrant-induced HR reduction was still present following combined sympathetic (atenolol) and parasympathetic (atropine) inhibition in dogs, as well as vagotomy in rats. Camizestrant reduced hHCN4 current density in Chinese hamster ovary cells, as well as beat rate and "funny" pacemaker (I_f) current activity in hESC-derived SAN cardiomyocytes. Camizestrant at 75 mg/kg for 7 days significantly reduced I_f current activity versus vehicle in isolated SAN cardiomyocytes. These results support the hypothesis that camizestrant exerts a pharmacologic, reversible reduction in HR by decreasing SAN pacemaker current activity.

1. Introduction

Selective estrogen receptor degraders (SERDs) are a class of endocrine therapy used in the treatment of estrogen receptor (ER)-positive breast cancer (Guglielmi et al., 2024). Camizestrant is a next-generation SERD and complete ER antagonist (Lawson et al., 2023) under Phase III development for the treatment of ER-positive/human epidermal growth factor receptor 2 (HER2)-negative breast cancer in the early (Hamilton et al., 2025) and advanced (André et al., 2022; Turner et al., 2023a) settings. Camizestrant has demonstrated a well-tolerated, dose-

Abbreviations: ANOVA, Analysis of variance; Bpm, Beats per min; CHO, Chinese hamster ovary; C_{max}, Maximum plasma concentration; ER, Estrogen receptor; HER2, Human epidermal growth factor receptor 2; hESC, Human embryonic stem cell; (h)HCN(4), (Human) hyperpolarization-activated cyclic nucleotide-gated channel (4); HR, Heart rate; IC_{50}, Half-maximal inhibitory concentration; I_f, "Funny" pacemaker current; IV, intravenous; SAN, Sinoatrial node; SERD, Selective estrogen receptor degrader..

* Corresponding author at: Clinical Pharmacology and Safety Sciences, R&D, AstraZeneca, Cambridge CB2 8PA, United Kingdom.
E-mail address: lindsay.wright@astrazeneca.com (L. Wright).

[1] At the time of study.

https://doi.org/10.1016/j.taap.2026.117804
Received 9 January 2026; Received in revised form 17 March 2026; Accepted 25 March 2026
Available online 27 March 2026

dependent safety profile and encouraging clinical activity as monotherapy and in combination with cyclin-dependent kinase 4/6 inhibitors or the AKT serine/threonine kinase (protein) inhibitor capivasertib (Oliveira et al., 2022; Turner et al., 2023b; Hamilton et al., 2024a; Oliveira et al., 2024; Vaklavas et al., 2024).

Prior to clinical development, experiments in dogs showed that camizestrant led to a gradual and reversible dose-dependent heart rate (HR) reduction. Subsequently, a reversible dose- and time-dependent reduction in resting HR was observed in patients with ER-positive/HER2-negative breast cancer receiving camizestrant (Hamilton et al., 2024a). At the Phase III dose of camizestrant 75 mg (André et al., 2022; Turner et al., 2023a; Hamilton et al., 2025), adverse events of bradycardia were typically asymptomatic and did not require dose adjustment (Hamilton et al., 2024a; Oliveira et al., 2024). Adverse events of bradycardia have also been reported in patients receiving the investigational SERDs giredestrant (Jhaveri et al., 2024) and imlunestrant (Jhaveri et al., 2025), and the investigational, selective ERα covalent antagonist H3B-6545 (Hamilton et al., 2024b). However, the approved SERDs fulvestrant and elacestrant are not associated with HR reduction (Ascione et al., 2024), suggesting that the effects of camizestrant on HR may be driven by an unknown, off-target mechanism.

Following these preclinical and clinical observations, experiments were conducted to examine the mechanism of camizestrant-induced HR reduction. It was hypothesized that camizestrant may act similarly to ivabradine, a known hyperpolarization-activated cyclic nucleotide-gated channel (HCN) inhibitor that acts on the sinoatrial node (SAN; the natural pacemaker of the heart (Kashou et al., 2022)), to cause HR reduction by inhibiting the cardiac pacemaker channel (Bucchi et al., 2006). Data in nonclinical cardiac models are presented here, including both the initial telemetry experiments (in dogs) that preceded clinical development and the subsequent in vivo and in vitro investigations, to further examine the effects of camizestrant on HR and the associated mechanisms.

2. Materials and methods

Procedures were approved by the local ethics/animal use committees and were conducted in accordance with the relevant local guidelines, the details of which are provided in the supplementary data.

2.1. Cardiovascular telemetry experiments in dogs

Male and female beagle dogs supplied by Envigo RMS (UK) Limited, Bicester, Oxfordshire, UK, or Marshall BioResources, UK, were used as a standard non-rodent model to study drug effects on the cardiovascular system.

Two cardiovascular telemetry studies were performed with administration of camizestrant at 5–20 mg/kg for 7 or 28 days once daily by oral gavage. Additional experiments examined the effects of chronotropic agents (administered as single doses) and exercise. Atenolol at 10 mg/kg was administered by oral gavage, while glycopyrrolate at 30 μg/kg and atropine at 100 μg/kg were each administered as an intravenous (IV) bolus. For isoprenaline experiments, isoprenaline at 0.2 and 0.4 μg/kg/min, and saline, were administered by IV infusion for 10 min each. Interventions commenced nominally 2 h following vehicle (deionized purified water; pH adjusted to 4.8–5.5 with 1 N HCl) or camizestrant administration; atropine was administered 2 h following atenolol administration.

2.2. Cardiovascular telemetry experiments in rats

Male Han Wistar rats at least 7 weeks old (supplied by Charles River, Margate, UK) were used as a standard rodent model to study the effects of camizestrant on HR.

Rats were dosed once daily by oral gavage with vehicle (0.5% hydroxypropyl methylcellulose), then with camizestrant 75 mg/kg for 7 days at a dose volume of 10 mL/kg. The HR of the animals was monitored by telemetry (blood pressure waveform) for at least 1 h pre-dose and for up to 22 h post-dose on Dosing Day [D]1, D3, D5, and D7.

A vagotomy study was performed on male rats ($n = 5$/group) dosed once daily by oral gavage with vehicle (deionized purified water; pH adjusted to 4.8–5.5 with 1 N HCl) or camizestrant 75 mg/kg for 4 days at a dose volume of 10 mL/kg. HR was monitored by telemetry (blood pressure waveform) for approximately 1 h pre-dose and up to 22 h post-dose on Dosing D1, D2, and D3 and until termination on Dosing D4.

2.3. In vivo exposure

Samples to calculate plasma exposure of camizestrant were collected during the telemetry studies.

2.4. Chinese hamster ovary cell line stably expressing human HCN4

Chinese hamster ovary (CHO) cells (Cytomyx, Cambridge, UK) stably transfected with recombinant human HCN 4 (hHCN4) were cultured. Cells were treated with camizestrant or ivabradine (used as a positive control of HCN4 blockade (Bucchi et al., 2006)).

2.5. Human embryonic stem cell-derived SAN cardiomyocytes

The protocol for the directed differentiation of human embryonic stem cells (hESCs) into SAN cardiomyocytes used here has been previously described in detail (Protze et al., 2017).

The effect of camizestrant on beat rate was measured every 24 h for 7 days using the xCELLigence RTCA CardioECR impedance platform (Agilent Technologies, California, USA). After 24 h of exposure to treatment, and every 24 h thereafter, data on beat rate were collected via sets of 11× 45-s sweeps initiated every 3 min across a 30-min period. During the first 48 h, data were also recorded hourly to determine the time profile of any changes in beat rate.

Patch-clamp experiments were performed after a beating cell monolayer had formed, usually 72 h post-plating (Suppl Table S1; Suppl Fig. S1). After a giga-ohm seal and perforation had occurred, a current recording was made.

2.6. Primary rat SAN cardiomyocytes

Male Han Wistar rats 8–9 weeks old (Charles River) were used for isolation of primary rat SAN cardiomyocytes.

For acute in vitro experiments, camizestrant was dissolved in dimethyl sulfoxide to a 30 mM stock and subsequently diluted in Tyrode's solution (supplemented with 1 mM $BaCl_2$ and 2 mM $MnCl_2$ to better dissect the “funny” pacemaker current [I_f current]) to the concentrations indicated in figure legends; concentrations were then delivered in the recording in vitro chamber. Camizestrant for in vivo treatments was administered to the animals by oral gavage at a concentration of 7.5 mg/mL and a volume of 10 mL/kg to achieve a final dose of 75 mg/kg. The vehicle was deionized water adjusted to pH 4.8–5.5.

2.7. Statistical analysis

Details of specific statistical tests can be found in the supplementary data. Statistical significance was set at $p < 0.05$ for all in vivo and in vitro experiments.

3. Results

3.1. Camizestrant causes a dose- and time-dependent reduction in HR in vivo in dogs and rats

An initial preclinical 7-day administration study in male beagle dogs

suggested a time-dependent reduction in HR, with a maximum decrease in HR for camizestrant versus vehicle of 40 beats per min (bpm; 107.4 bpm vehicle vs 67.7 bpm camizestrant 10 mg/kg; 37%; $p < 0.001$) on D5 following daily administration of camizestrant 10 mg/kg (Fig. 1A,B; Suppl Table S2). The unbound maximum plasma concentration (C_{max}) on D4 was 0.45 μM (Suppl Table S3).

A subsequent 28-day administration study in male and female dogs examined responses to a range of camizestrant doses while on treatment and following recovery. A dose- and time-dependent reduction of HR was noted versus vehicle and pre-study levels (Fig. 1C,D; Suppl Table S4). The maximum HR reduction from pre-study levels (53 bpm reduction from a pre-study HR of 128 bpm, $p < 0.001$ vs vehicle) was noted with the maximum dose of camizestrant 20 mg/kg 1 h post-dose on D25. The unbound C_{max} on D28 for the doses of 5 mg/kg, 10 mg/kg, and 20 mg/kg was 0.18 μM, 0.44 μM, and 1.23 μM, respectively (Suppl Table S3). The observed effect was reversible, as the HR for dogs in the group receiving camizestrant 20 mg/kg reached similar levels to vehicle during recovery (D31 and D50, which represent 3 days and 22 days following cessation of treatment, respectively; Fig. 1C,D; Suppl Table S4).

Further experiments demonstrated HR reduction versus vehicle in rats receiving a daily dose of camizestrant 75 mg/kg (Fig. 1E,F), confirming an effect on HR in a second species. Specifically, a decrease in HR was noted during the dark phase on D1 and between 0 and 22 h post-dose on D3, D5, and D7, with a maximum decrease in HR for camizestrant versus vehicle of 65 bpm (16%; $p < 0.001$) on D1, 72 bpm (11%) on D3, 89 bpm (23%) on D5, and 132 bpm (16%; $p < 0.001$) on D7 (Suppl Table S5). The unbound C_{max} on D4 was 0.63 μM (Suppl Table S3).

3.2. Camizestrant effect on responses to chronotropic agents and exercise in dogs

IV infusion of isoprenaline 0.2 μg/kg/min for 10 min led to an increase in HR in dogs treated with camizestrant, although increases were dampened compared with vehicle (increase of 23 bpm [37%] vs 82 bpm [86%] for vehicle; Fig. 2A; both $p < 0.05$ vs respective IV saline dose). Infusion of isoprenaline 0.4 μg/kg/min for 10 min led to a similar increase in HR in the presence of camizestrant to that seen for 0.2 μg/kg/min (increase of 29 bpm [40%]; Fig. 2A; $p < 0.05$ vs vehicle). Glycopyrrolate 30 μg/kg and atropine 100 μg/kg caused HR increases in camizestrant-treated animals, although increases were dampened compared with vehicle (Fig. 2B). At 4 days following cessation of treatment with camizestrant 20 mg/kg/day, rechallenge with glycopyrrolate 30 μg/kg caused an HR increase of 114% (194 bpm) versus baseline, showing a recovery of HR increase compared with pre-dose. Endogenous stimulation by 15-min exercise resulted in a similar HR increase for vehicle and camizestrant (increased by 75 bpm [72%] and 60 bpm [115%], respectively; Fig. 2C), although the mean HR was lower for camizestrant (112 bpm) versus vehicle (178 bpm); of note, the baseline HR levels pre-intervention were already reduced in the camizestrant-treated group.

3.3. The autonomic nervous system does not appear to mediate camizestrant effects

To determine whether HR reduction with camizestrant was the result of autonomic tone changes, the influence of sympathetic effects on HR was inhibited in conscious dogs by oral dosing with atenolol 10 mg/kg (a β-adrenergic receptor antagonist) and, 2 h later, IV atropine 100 μg/kg

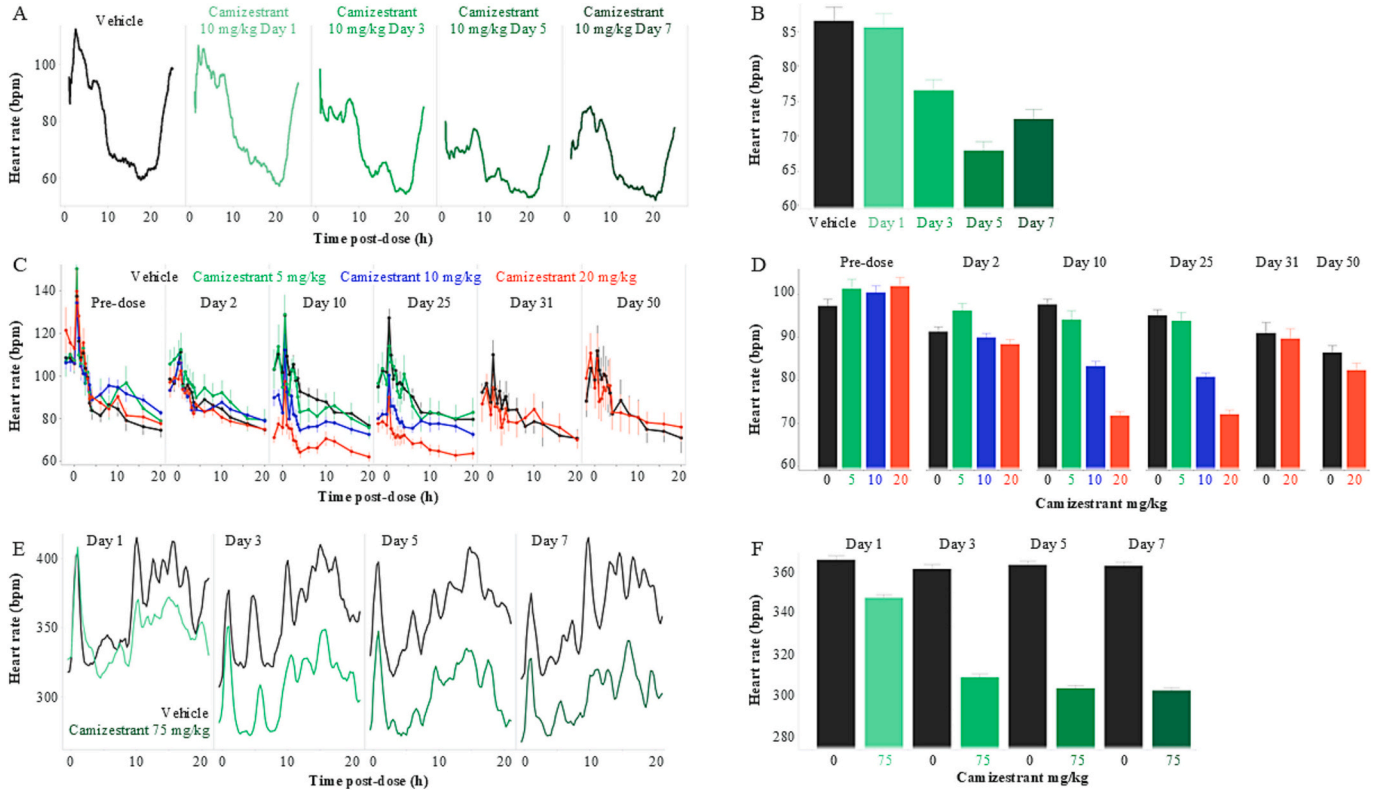

Fig. 1. Time course of heart rate (HR) reduction in camizestrant-treated animals. (A) HR in telemetered dogs after a single day of treatment with vehicle (baseline) followed by 7 days of daily doses of camizestrant 10 mg/kg ($n = 4$). (B) Mean 24-h HRs for data shown in (A). (C) HR in telemetered dogs following 28 days of daily doses with vehicle or camizestrant (pre-study and Day (D)2, D10, and D25: control, $n = 10$; camizestrant 5 mg/kg, $n = 6$; camizestrant 10 mg/kg, $n = 6$; camizestrant 20 mg/kg, $n = 10$; D31 and D50: control, $n = 4$; camizestrant 20 mg/kg, $n = 4$). (D) Mean 24-h heart rates for data shown in panel C. (E) HR in telemetered rats following 7 days of daily doses with vehicle or camizestrant 75 mg/kg ($n = 8$). (F) Mean 24-h heart rates for data shown in panel E. Data are mean ± standard error of the mean.

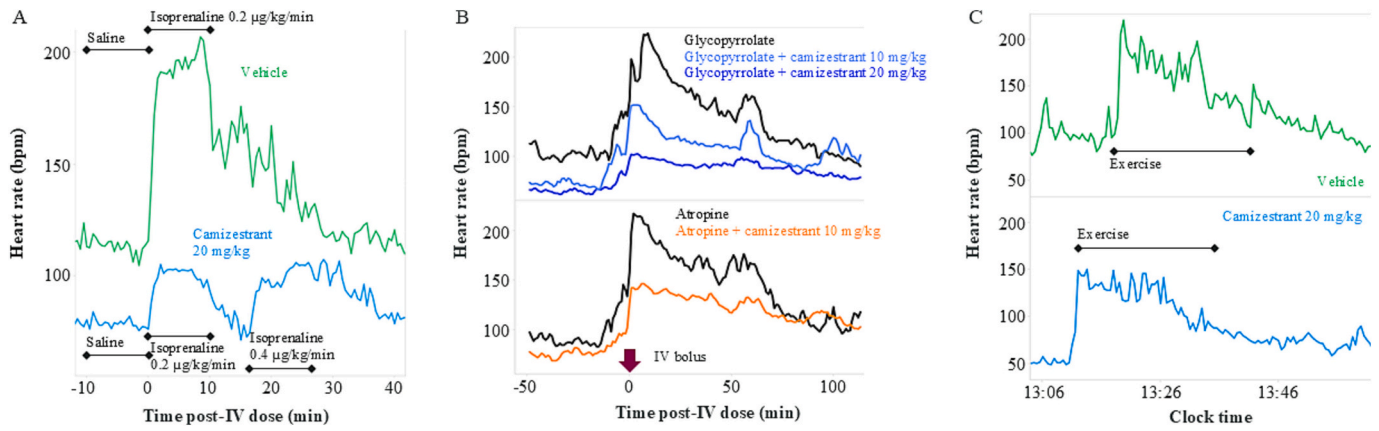

Fig. 2. Responsiveness to chronotropic stimulation in camizestrant-treated dogs. (A) Heart rate (HR) in conscious dogs ($n = 3$) in response to isoprenaline prior to and following 7 days of dosing with camizestrant 20 mg/kg. (B) HR in conscious dogs ($n = 3$) in response to glycopyrrolate 30 µg/kg (top panel) and atropine 100 µg/kg (bottom panel) prior to and following 7 days of dosing with camizestrant 10 or 20 mg/kg. (C) HR in conscious dogs ($n = 3$) in response to 15 min of exercise (social interaction/active play) prior to and following 7 days of dosing with camizestrant. Data are means.

(a muscarinic receptor antagonist that blocks parasympathetic effects) was administered. This combination is expected to decrease the autonomic influence on HR (Silva et al., 2017). This autonomic block procedure was performed on dogs initially treated with vehicle, and then in the same dogs after 14 days' dosing with camizestrant 10 mg/kg. Fig. 3B shows HR following atenolol dosing, demonstrating that HR is lower following camizestrant treatment. Fig. 3C shows the effects of atropine on HR when administered 2 h after atenolol. Camizestrant-induced HR reduction was still present following combined sympathetic and parasympathetic inhibition.

Experiments were performed in rats pre- and post-vagotomy to further interrogate autonomic nervous system involvement in camizestrant-induced HR reduction. Following treatment with camizestrant 75 mg/kg, a decrease in HR was observed from 3 h post-dose on D2 and throughout the 22-h recording period on D3, with a maximum decrease versus vehicle of 87 bpm (22%) (Suppl Fig. S2). Following anesthesia on D4, the HR reduction with camizestrant was still evident, with a maximum decrease versus vehicle of 54 bpm (12%; Fig. 3D; $p < 0.001$). The HR decrease was still present after vagotomy, with a maximum decrease versus vehicle of 82 bpm (19%) in camizestrant-treated animals (Fig. 3D; Suppl Table S6; $p < 0.01$). Before the vagotomy procedure, phenylephrine infusion caused a baroreflex decrease in

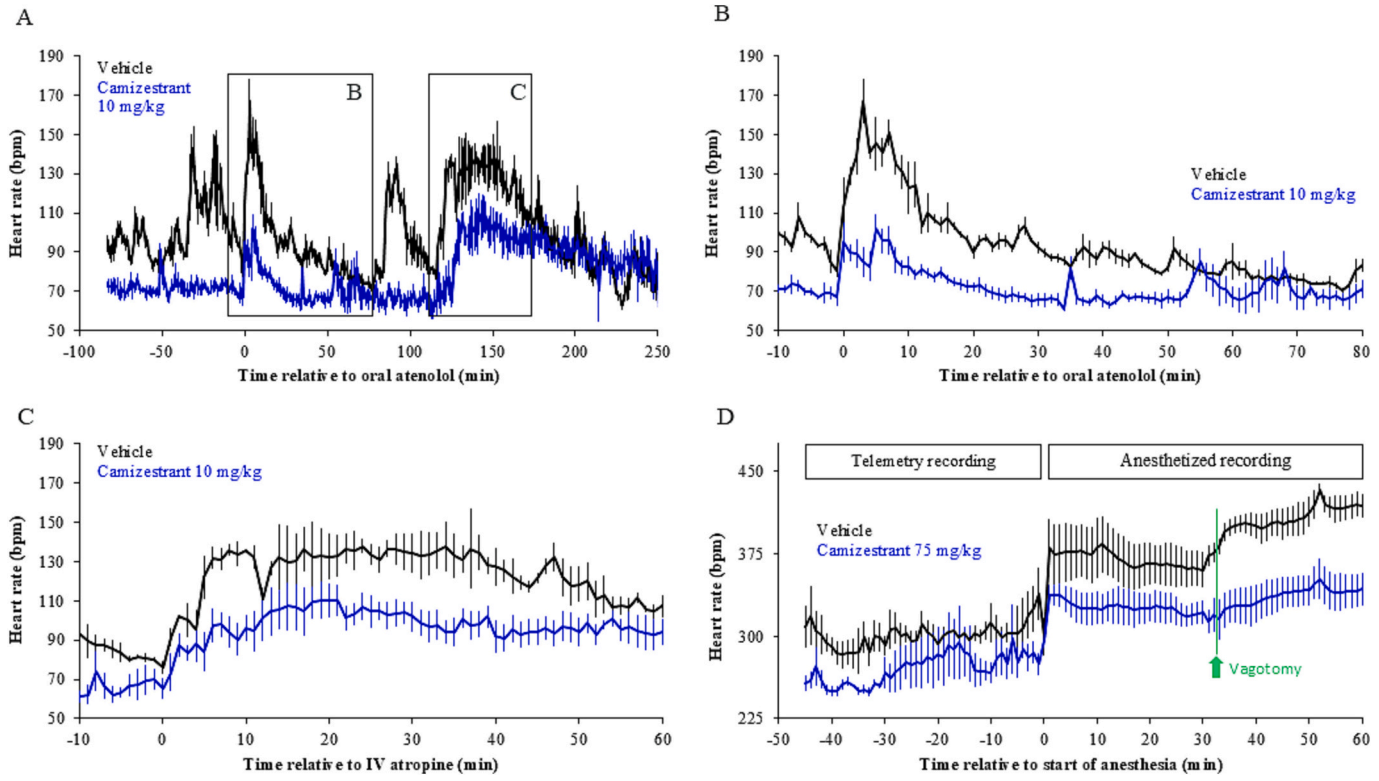

Fig. 3. Camizestrant-induced heart rate (HR) reduction is not mediated by autonomic involvement. Fig. shows HR in conscious dogs ($n = 3$) in response to oral atenolol 10 mg/kg prior to vehicle and following 7 days of dosing with camizestrant 10 mg/kg and intravenous atropine 100 µg/kg received 2 h after administration of atenolol. (A) The entirety of the telemetry time course. (B) and (C) Responses to atenolol and atropine. (D) HR in anesthetized rats ($n = 5$) before and after vagotomy following prior treatment with either vehicle or camizestrant 75 mg/kg. Data are mean ± standard error of the mean.

HR of 26 bpm and 24 bpm in the vehicle and camizestrant groups, respectively. Following the vagotomy, the phenylephrine-induced baroreflex decrease in HR was limited to 8 bpm and 10 bpm for the vehicle and camizestrant groups, respectively, confirming that the vagotomy was successful.

3.4. Camizestrant reduces HCN4 current density in hHCN4-expessing CHO cells

It was hypothesized that the effects of camizestrant on HR could be due to mechanisms involving the activity of pacemaker HCN4 channels in the SAN. Experiments were conducted initially in a CHO cell line stably expressing hHCN4 to study isolated pharmacologic effects; the HCN inhibitor ivabradine was used as a positive control (Bucchi et al., 2006). Acutely, ivabradine reduced hHCN4 current density in CHO cells, as expected (Fig. 4A; Suppl Table S7). Camizestrant reduced the hHCN4 current density by 24% at 50 μM when activated by a − 120 mV hyperpolarizing pulse (Fig. 4B; Suppl Table S7). However, the camizestrant effect was increased when hyperpolarizing the cell at −90 mV to reach a half-maximal inhibitory concentration (IC_{50}) of 14.2 μM (Fig. 4B; Suppl Table S7). Camizestrant treatment for 72 h exerted a dose-dependent decrease on the hHCN4 current at −110 mV (Fig. 4C), resulting in an IC_{50} of 2.5 μM (Fig. 4D). Camizestrant exerted a similar effect on the hHCN4 current at all voltage levels tested (Fig. 4E). Camizestrant at 10 μM significantly reduced the hHCN4 functional expression in a time-dependent manner as early as 6 h following incubation (Fig. 4F).

3.5. I_f current activity in hESC-derived SAN cardiomyocytes is decreased by camizestrant treatment

The effects of camizestrant in hESC-derived SAN cardiomyocytes, a physiological model of pacemaker channel function (Protze et al., 2017), were then examined. The I_f current inhibitors ivabradine and ZD7288 reduced beat rate in the hESC-derived SAN cells as expected (Fig. 5A; Suppl Table S8). Camizestrant reduced beat rate in a time- and concentration-dependent manner, with the effect plateauing at 48 h (Fig. 5B; Suppl Table S8).

Action potential recordings made in hESC-derived SAN cells by patch clamping (Fig. 5C,D) demonstrated that 48-h incubation with camizestrant significantly reduced the diastolic depolarization rate at 1 μM and 10 μM, leading to a reduction of 44% and 87% versus vehicle, respectively (Fig. 5E). Furthermore, treatment with camizestrant 10 μM reduced beat frequency by 40%, with no significant changes observed at lower concentrations (Fig. 5F,G). The differences in frequency rate observed in Fig. 5B,F are likely due to the different methods/temperatures of measuring beat rate. Measurements in Fig. 5A,B were made by impedance (xCELLigence RTCA CardioECR), which enables a noninvasive, label-free method for assessing beat rate within the controlled environment of an incubator (37 °C), while the more invasive patch-clamp experiments enable more cellular control and measurement of the I_f current and diastolic depolarization rate at room temperature.

A concentration-dependent decrease in cardiac pacemaker I_f current density was observed in cells treated with camizestrant versus vehicle for 72 h, with decreases of 24% at 0.01 μM, 56% at 0.1 μM, 71% at 1 μM, and 102% at 10 μM (Fig. 5H). Following incubation with 1 μM camizestrant versus vehicle for 24 h and 72 h, cardiac pacemaker I_f current density was reduced by 43% and 71%, respectively (Fig. 5I,J).

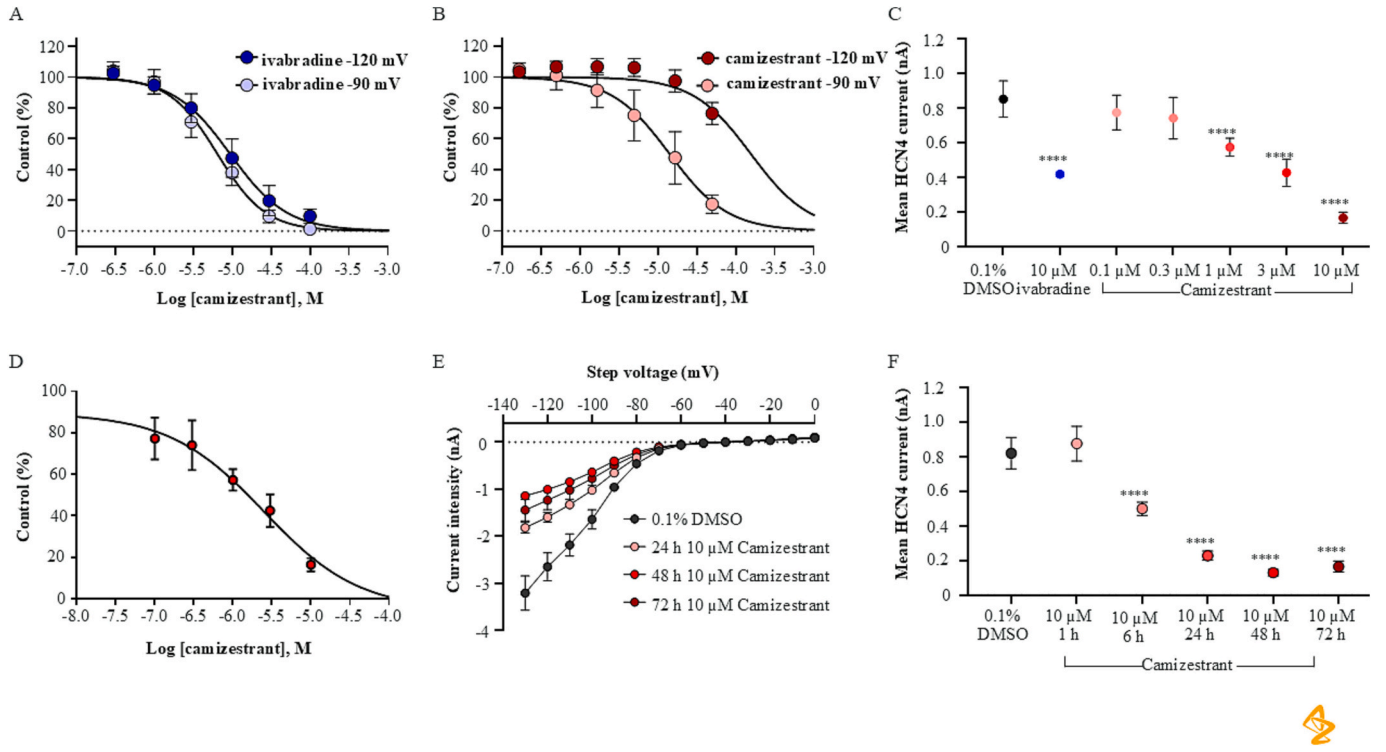

Fig. 4. Camizestrant causes a dose- and time-dependent decrease in hyperpolarization-activated cyclic nucleotide-gated channel 4 (HCN4) current in human HCN4 (hHCN4)-expressing Chinese hamster ovary cells. HCN4 current after treatment for a minimum of 3 min with (A) ivabradine at −90 mV ($n = 15$) and − 120 mV ($n = 8$) or (B) camizestrant at −90 mV ($n = 7$) and − 120 mV ($n = 7$) (QPatch™). (C) HCN4 current after 72 h of treatment with camizestrant or ivabradine ($n = 3$–9/group; IonWorks™). (D) HCN4 current after 72 h of treatment with camizestrant ($n = 4$–5; IonWorks). (E) Current–voltage relationship curve of HCN4 current after 10 μM camizestrant treatment ($n = 3$/group; QPatch). (F) HCN4 current after 10 μM camizestrant treatment ($n = 3$–8/group; IonWorks). (A), (B), and (E): data are mean ± standard error of the mean. ****$p < 0.0001$ versus vehicle by one-way analysis of variance (ANOVA) followed by Tukey's post hoc test.

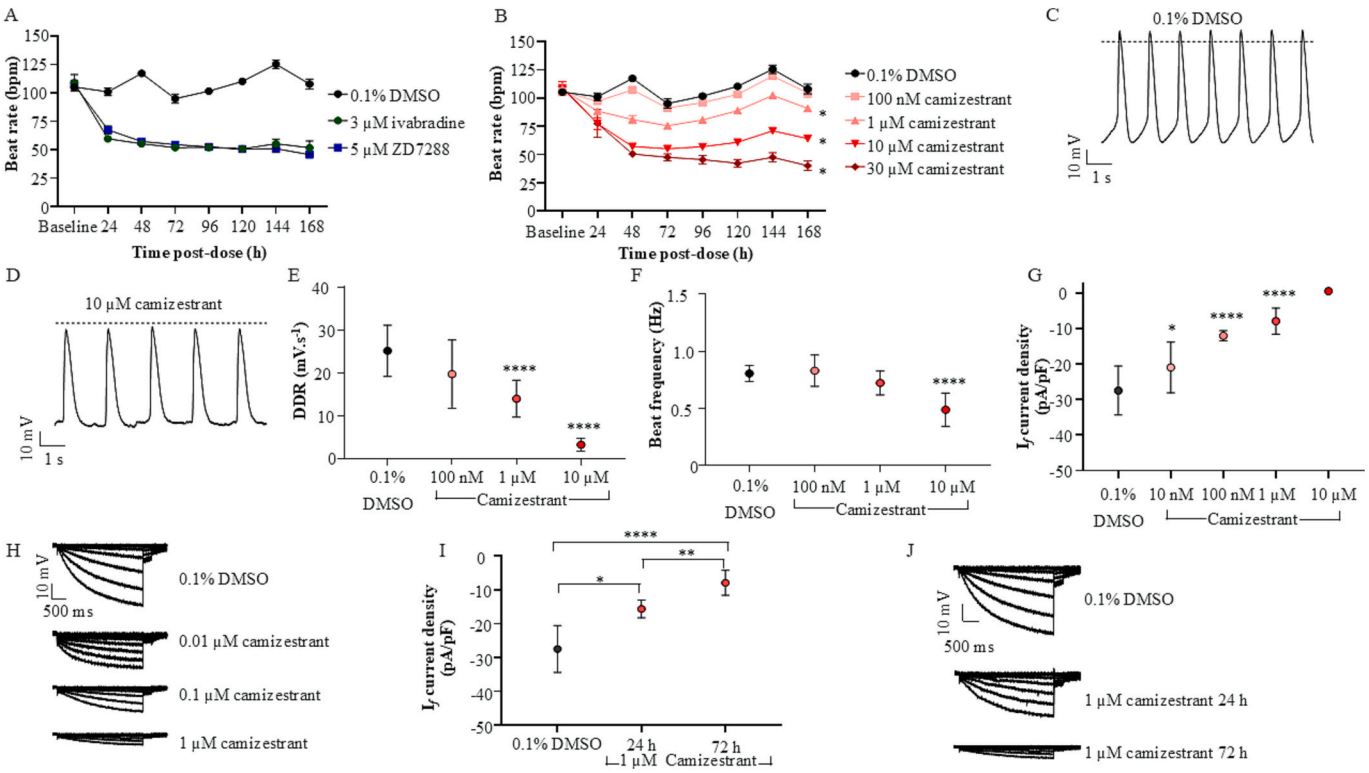

Fig. 5. Camizestrant effects in human embryonic stem cell-derived sinoatrial node cardiomyocytes. Beat rate after 48 h of treatment with (A) ivabradine or ZD7288 ($n = 2$/group) or (B) camizestrant ($n = 4$/group). (C) and (D) Representative action potential traces. (E) DDR after 48 h of camizestrant treatment ($n = 5$–14/group). (F) Beating frequency after 48 h of camizestrant treatment ($n = 5$–15/group). (G) "Funny" pacemaker current (I_f current) density after 72 h of camizestrant treatment ($n = 1$–11/group). (H) Representative I_f current traces. (I) I_f current density after 24 h of vehicle, or after 24 h or 72 h of camizestrant treatment ($n = 3$–10/group). (J) Representative I_f current traces. (A) and (B): data are mean ± standard error of the mean. (E), (F), (G), and (I): data are mean ± standard deviation. $^*p < 0.05$, $^{**}p < 0.01$, $^{****}p < 0.0001$ vs vehicle by one-way analysis of variance (ANOVA) followed by Tukey's post hoc test.

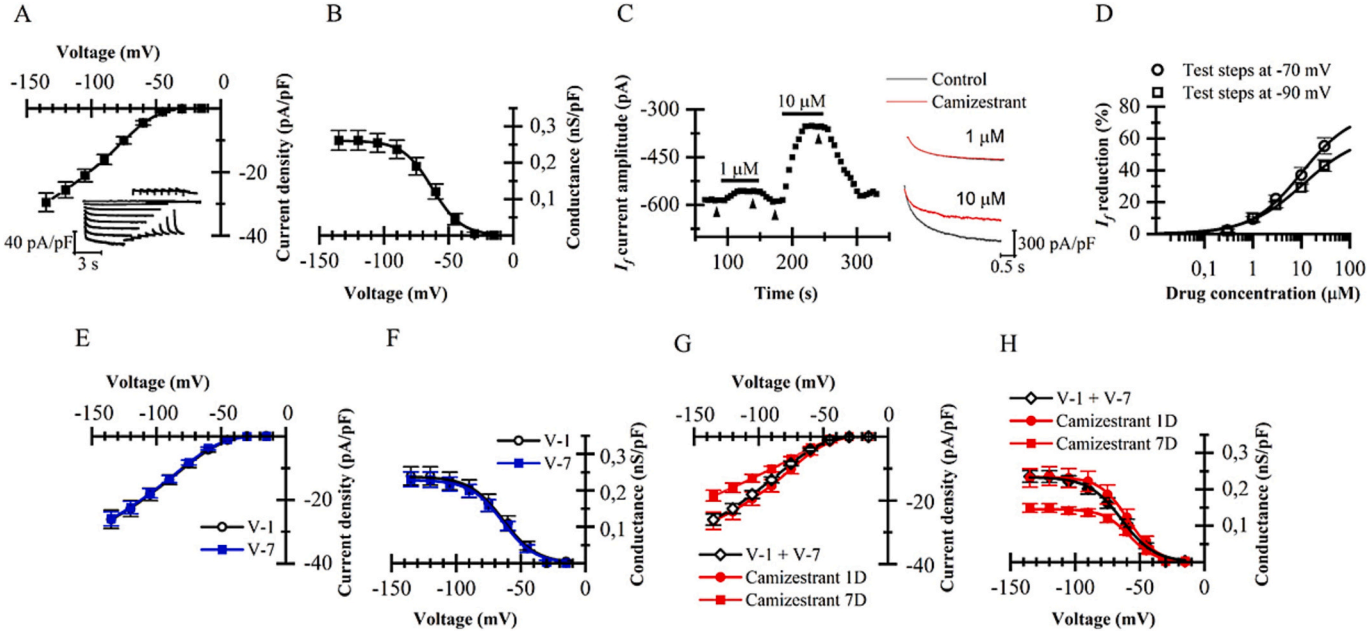

Fig. 6. Camizestrant reduces pacemaker current parameters in primary rat sinoatrial node cardiomyocytes. (A) Current density/voltage curve ($n = 19$). (B) Conductance/voltage curve ($n = 19$). (C) Left: representative time course of "funny" pacemaker current (I_f current) amplitude before, during, and after perfusion of camizestrant at 1 μM and 10 μM; right: representative I_f current traces collected in correspondence to arrows on the left. (D) Dose–response curve of camizestrant-induced I_f current density reduction at −70 mV and − 90 mV. (E) Current density/voltage ($n = 13$) and (F) conductance/voltage ($n = 13$) curves after one and seven daily vehicle administrations. (G) Current density/voltage ($n = 15$) and (H) conductance/voltage ($n = 15$) curves after one camizestrant administration (AZ-1D). (A), (B), (D), (E), (F), (G), and (H): data are mean ± standard error of the mean.

3.6. I_f current activity in primary rat SAN cardiomyocytes

The effects of prolonged in vivo administration of camizestrant on the cardiac pacemaker I_f current recorded from single rat SAN cardiomyocytes were then tested. The presence of the current was confirmed and the voltage dependence of the steady-state current density, and of the conductance, were characterized (Fig. 6A,B; Suppl Table S9). In cells isolated from nontreated animals, acute exposure to camizestrant (1 μM and 10 μM) elicited fast and fully reversible dose-dependent reductions of the I_f current (mean reduction of 9% and 37% for 1 μM and 10 μM, respectively; sample time course and current traces in Fig. 6C; Suppl Table S10). Several doses were evaluated using two different test potentials (−70 mV and − 90 mV; Fig. 6D, Suppl Table S11) with an IC_{50} (at −70 mV) of 10.3 μM.

Next, SAN cells were isolated from rats treated with vehicle or camizestrant 75 mg/kg for 1 or 7 consecutive days. The vehicle did not induce any modification in current density (Fig. 6E; $p = 0.9972$) or conductance (Fig. 6F; $p = 0.8795$; Suppl Table S12) after 1 or 7 days of exposure; thus, vehicle data were pooled together (Fig. 6G,H; Suppl Table S12). Exposure to camizestrant for 1 day did not affect current density (Fig. 6G; extra sum-of-squares F-test; $p = 0.5352$) or maximal conductance (Fig. 6H; extra sum-of-squares F-test; $p = 0.841$). However, a significant shift of the Boltzmann fitting of the conductance curve was observed (+4.87 mV; extra sum-of-squares F-test; $p < 0.0001$).

Prolonged (7-day) camizestrant exposure significantly reduced the maximal conductance versus vehicle and versus 1 day of exposure (by 37.7% and 37.8%, respectively; $p < 0.0001$; Fig. 6G,H; Suppl Tables S12,S13). Additionally, prolonged exposure significantly shifted the voltage dependence of the conductance curve versus vehicle only (+5.85 mV; extra sum-of-squares F-test; $p < 0.0001$; Suppl Table S13).

4. Discussion

Treatment-related adverse events of bradycardia have been reported in patients with breast cancer receiving camizestrant (Hamilton et al., 2024a); therefore, the hypothesis that camizestrant causes HR reduction by a pacemaker channel-mediated mechanism in the SAN was tested.

The data favor the hypothesis of a pacemaker channel-mediated mechanism. In dogs, atropine, isoprenaline, and glycopyrrolate (agents acting to increase HR in the SAN) elicited an increase in HR, but the absolute peak HR was reduced by camizestrant treatment (vs vehicle), indicating that camizestrant may exert a biological effect on HR reduction in the SAN. Similarly, in the case of exercise-induced HR increase, the absolute peak HR was reduced by camizestrant treatment, but relative response versus baseline was not dampened versus vehicle-treated dogs, suggesting that stimuli with pleiotropic effects on cardiac function may exert a robust increase in HR irrespective of camizestrant treatment. Furthermore, in vivo experiments in both dogs and rats supported that camizestrant-induced HR reduction is not mediated by effects on the autonomic nervous system. Following vagotomy in rats to ablate the actions of the vagus nerve (the main parasympathetic branch of the autonomic nervous system which can induce HR reduction via negative chronotropic action on the SAN (Capilupi et al., 2020)), a sustained decrease in HR induced by camizestrant was not attenuated. Additionally, consecutive sympathetic block by atenolol (Montano et al., 1998) and parasympathetic block by atropine (Montano et al., 1998) in dogs led to similar relative effects on HR in the presence or absence of camizestrant treatment, further supporting that camizestrant does not exert a marked effect on autonomic tone. In vitro, in hESC-derived SAN cardiomyocytes, camizestrant reduced the beat rate and diastolic depolarization rate of the action potential, one of the main key drivers of automaticity in these cells (Turner et al., 2021). Camizestrant also reduced the pacemaker current recorded from two different cell models: HCN current recorded from CHO cells overexpressing hHCN4, and I_f current recorded from the more physiologically relevant hESC-derived SAN cardiomyocytes. Hence, camizestrant action on native SAN cells could also be mediated by a reduction on the functional expression of the cardiac pacemaker I_f current. Finally, in rats treated with a camizestrant dose known to cause HR reduction, the I_f current recorded from isolated SAN cells was reduced, demonstrating that camizestrant reduced the I_f current in both in vitro and in vivo models (Central Illustration).

These data support the hypothesis that camizestrant acts in a similar manner to ivabradine to reduce HR. However, unlike camizestrant, ivabradine exerts an effect by directly blocking HCN channels (Bucchi et al., 2006), which are molecular correlates of the I_f current regulating neuronal excitability and the autonomous rhythm of the heart (Hennis et al., 2022). The HCN4 isoform is the predominant subtype in the SAN; in the absence of HCN4 regulation, the electrical activity of the SAN becomes unstable, resulting, among others, in HR reduction (Hennis et al., 2022). Although there is some evidence that camizestrant can also directly block HCN channels at high concentrations, the delayed onset of the effect reported renders decreased HCN activity as a more likely driver of camizestrant-induced HR reduction, possibly by reduced cell membrane expression of cardiac pacemaker channels. Indeed, in this study, camizestrant reduced the amount of HCN4 current recorded from hHCN4-expressing CHO cells, with minimal effect at 1 h and peak reduction following 48-h incubation. A similar delayed-onset effect was observed on beat rate and pacemaker I_f current density recorded from hESC-derived SAN cardiomyocytes. Finally, SAN cells isolated from rats treated with camizestrant showed a reduction in I_f current density after 7 days of treatment, but not after 1 day of treatment. There are other examples where downregulation of HCN4 is linked to HR reduction: HCN4 has been implicated in HR reduction induced by the receptor tyrosine kinase inhibitor crizotinib (Zhang et al., 2017), but it is unlikely that the involved mechanisms would overlap with those for camizestrant. Downregulation of the HCN4 channel and the corresponding I_f current has also been proposed to underlie exercise-induced HR reduction in rodents and humans, in this case via genetic regulation mechanisms (D'Souza et al., 2014; D'Souza et al., 2017).

Certain translational aspects of the data reported should be highlighted. Camizestrant is associated with a reversible dose- and time-dependent reduction in resting HR in patients with breast cancer, with a gradual decrease to a stable minimum over ~14 days and recovery to baseline following treatment end, with a profile broadly symmetrical to the onset profile; exercise-induced increases in HR were reported as possible in patients (Hamilton et al., 2024a). This delayed-onset effect is also evident in the nonclinical data in rats and dogs, as the peak HR reduction was reached at ~7 days in rats and at 5–10 days in dogs. A reversible, dose-dependent HR reduction was demonstrated in dogs, and exercise-induced increases in HR were possible, reflecting the published clinical data in patients with breast cancer (Hamilton et al., 2024a). The in vitro data collected from hHCN4-expressing CHO cells and hESC-derived SAN cardiomyocytes also indicated that the effects of camizestrant are delayed in onset, as well as being concentration dependent. Additionally, in patients with breast cancer, HR reduction at the 75 mg and 150 mg doses (maximum reduction of 12.5 bpm and 13.5 bpm, respectively) was observed at unbound C_{max} values of 0.034 μM and 0.086 μM, respectively (Hamilton et al., 2024a). These concentrations closely align with the lowest concentration of 0.01 μM camizestrant that reduced pacemaker I_f current density by 24% in hESC-derived SAN cardiomyocytes. Interestingly, when compared with clinical data, the HR reduction observed in rats and dogs occurred at higher unbound C_{max} values ranging from 0.18 μM to 1.23 μM, suggesting that the effect of camizestrant in humans may be more potent compared with that in nonclinical species. However, as the phenomenon of dose-dependent and delayed-onset effect is shared between nonclinical models and humans, a common mechanism potentially underlies HR reduction across species.

There are several limitations relating to this study. First, the molecular and cellular mechanisms of the camizestrant-induced reduction of cardiac pacemaker I_f current density in the SAN were not further dissected. These could involve direct or indirect interaction or

phosphorylation of the channels, modulation of trafficking, or genetic regulation of expression. These data do indicate that camizestrant binds the HCN4 channel and acutely inhibits the I_f current in rat-isolated SAN cells. However, whether this acute binding is linked to subsequent delayed-onset reduction in I_f current density remains unknown. Additionally, as only the activity of HCN4 (the predominant isoform in the SAN (Shi et al., 1999)) was investigated, it cannot be excluded that camizestrant may affect other HCN isoforms. Future work could investigate the specific mechanism by which camizestrant inhibits HCN4/I_f current.

Moreover, the contribution of ER degradation and antagonism (the primary target for camizestrant) to HR reduction was not interrogated. Evidence suggests this is unlikely, as other SERDs such as fulvestrant and elacestrant are not associated with HR reduction (Ascione et al., 2024). It is also worth noting that HR reduction was observed in both male and female dogs treated with camizestrant, suggesting that sex hormone interruption may not be a contributing mechanism. However, a potential link between action on the ER and HR reduction cannot be ruled out based on the data reported here. There is some literature linking estrogen signaling with HR; for example, 17β-estradiol has been shown to accelerate SAN automaticity by increased I_f density mediated by ERα in pregnant mice (Long and Fiset, 2020). Giredestrant is also associated with a delayed-onset HR reduction (Brooks et al., 2023). Therefore, the link between ER activity and HR reduction requires further investigation.

Finally, surgical vagotomy alone does not assess the role of the entire autonomic nervous system; further experiments involving surgical sympathectomy or stellate ganglion ablation would be needed to fully rule out effects mediated by the sympathetic nervous system.

5. Conclusions

Overall, data from the nonclinical in vivo and in vitro investigations reported here indicate that camizestrant exerts a pharmacologic, reversible effect on HR mediated via a pacemaker I_f current-dependent mechanism in SAN cardiomyocytes.

CRediT authorship contribution statement

Andrew Hall: Writing – review & editing, Writing – original draft, Visualization, Validation, Supervision, Project administration, Formal analysis, Data curation, Conceptualization. **Saïd El-Haou:** Writing – review & editing, Writing – original draft, Methodology, Investigation. **Inmaculada C. Villar:** Writing – review & editing, Writing – original draft. **David Molla:** Writing – review & editing, Writing – original draft. **Maggie Kwan:** Writing – review & editing, Writing – original draft. **Stuart Purbrick:** Writing – review & editing, Writing – original draft, Validation, Supervision, Project administration, Investigation. **David Henry:** Writing – review & editing, Writing – original draft. **Jason Kirk:** Writing – review & editing, Writing – original draft. **Glen Hawthorne:** Writing – review & editing, Writing – original draft, Supervision, Investigation. **Serena Canzolino:** Writing – review & editing, Writing – original draft. **Joanna Harding:** Writing – review & editing, Writing – original draft. **Alexander Harmer:** Writing – review & editing, Writing – original draft, Visualization, Validation, Supervision, Project administration, Formal analysis, Data curation, Conceptualization. **Annalisa Bucchi:** Writing – review & editing, Writing – original draft. **Liz Roberts:** Writing – review & editing, Writing – original draft, Methodology, Investigation. **Amy Pointon:** Writing – review & editing, Writing – original draft. **Stephanie Protze:** Writing – review & editing, Writing – original draft. **Mirko Baruscotti:** Writing – review & editing, Writing – original draft. **Lindsay Wright:** Writing – review & editing, Writing – original draft, Validation, Project administration, Formal analysis, Data curation, Conceptualization.

Funding

These studies were funded by AstraZeneca.

Declaration of competing interest

The authors declare the following financial interests/personal relationships which may be considered as potential competing interests:

David Molla received institutional funding to The Cell Physiology MiLab from AstraZeneca for their involvement in and resources for this study. Serena Canzolino received institutional funding to The Cell Physiology MiLab from AstraZeneca for their involvement in and resources for this study. Annalisa Bucchi received institutional funding to The Cell Physiology MiLab from AstraZeneca for their involvement in and resources for this study. Mirko Baruscotti received institutional funding to The Cell Physiology MiLab from AstraZeneca for their involvement in and resources for this study. Stephanie Protze has received an institutional research grant from the Canadian Foundation for Innovation and funding from AstraZeneca for their involvement in and resources for this study, personal consulting fees from BlueRock Therapeutics LP, and discloses a patent (patent no. WO2016131137; granted/issued in 2017). Andrew Hall reports a relationship with AstraZeneca that includes: employment and equity or stocks. Said El-Haou reports a relationship with AstraZeneca that includes: employment and equity or stocks. Inmaculada C. Villar reports a relationship with AstraZeneca that includes: employment and equity or stocks. Stuart Purbrick reports a relationship with AstraZeneca that includes: employment and equity or stocks. David Henry reports a relationship with AstraZeneca that includes: employment and equity or stocks. Jason Kirk reports a relationship with AstraZeneca that includes: employment and equity or stocks. Glen Hawthorne reports a relationship with AstraZeneca that includes: employment and equity or stocks. Alexander Harmer reports a relationship with AstraZeneca that includes: employment and equity or stocks. Liz Roberts reports a relationship with AstraZeneca that includes: employment and equity or stocks. Amy Pointon reports a relationship with AstraZeneca that includes: employment and equity or stocks. Lindsay Wright reports a relationship with AstraZeneca that includes: employment and equity or stocks. If there are other authors, they declare that they have no known competing financial interests or personal relationships that could have appeared to influence the work reported in this paper.

Acknowledgements

These studies were funded by AstraZeneca. The authors wish to thank Nick Edmunds, Stefan Kavanagh, Paul Morgan, Mike Rolf, and Pradeep Sharma for their helpful discussions and advice. Medical writing assistance, under the direction of the authors, was provided by Stavroula Bitsi, PhD, and Imogen Allred, PhD, of BOLDSCIENCE, funded by AstraZeneca in accordance with Good Publication Practice 2022 guidelines.

Appendix A. Supplementary data

Supplementary data to this article can be found online at https://doi.org/10.1016/j.taap.2026.117804.

Data availability

Data underlying the findings described in this manuscript may be obtained in accordance with the sponsor's data sharing policy described at https://astrazenecagrouptrials.pharmacm.com/ST/Submission/Disclosure. Data can be requested through Vivli at https://vivli.org/members/enquiries-about-studies-not-listed-on-the-vivli-platform/. The sponsor's Vivli member page is also available outlining further details: https://vivli.org/ourmember/astrazeneca/.

References

André, F., Im, S.A., Neven, P., Baird, R.D., Ettl, J., Goetz, M.P., Hamilton, E., Iwata, H., Jiang, Z., Joy, A.A., Haddad, V., Walding, A., Miralles, M.S., Bartlett, C.H., Llombart-Cussac, A., 2022. Abstract OT2-11-06: SERENA-4: a phase III comparison of AZD9833 (camizestrant) plus palbociclib, versus anastrozole plus palbociclib, for patients with ER-positive/HER2-negative advanced breast cancer who have not previously received systemic treatment for advanced disease (abstr). Cancer Res. 82. OT2-11-06.

Ascione, L., Castellano, G., Curigliano, G., Zagami, P., 2024. Endocrine therapy for early breast cancer in the era of oral selective estrogen receptor degraders: challenges and future perspectives. Curr. Opin. Oncol. 36, 465–473.

Brooks, L., Dolton, M., Langenhorst, J., Yoshida, K., Lien, Y.T.K., Malhi, V., Li, C., Perez-Moreno, P., Bond, J., Chen, Y.C., Yu, J., 2023. Concentration QTc analysis of giredestrant: overcoming QT/heart rate confounding in the presence of drug-induced heart rate changes. Clin. Transl. Sci. 16, 823–834.

Bucchi, A., Tognati, A., Milanesi, R., Baruscotti, M., DiFrancesco, D., 2006. Properties of ivabradine-induced block of HCN1 and HCN4 pacemaker channels. J. Physiol. 572, 335–346.

Capilupi, M.J., Kerath, S.M., Becker, L.B., 2020. Vagus nerve stimulation and the cardiovascular system. Cold Spring Harb. Perspect. Med. 10, a034173.

D'Souza, A., Bucchi, A., Johnsen, A.B., Logantha, S.J., Monfredi, O., Yanni, J., Prehar, S., Hart, G., Cartwright, E., Wisloff, U., Dobryznski, H., DiFrancesco, D., Morris, G.M., Boyett, M.R., 2014. Exercise training reduces resting heart rate via downregulation of the funny channel HCN4. Nat. Commun. 5, 3775.

D'Souza, A., Pearman, C.M., Wang, Y., Nakao, S., Logantha, S., Cox, C., Bennett, H., Zhang, Y., Johnsen, A.B., Linscheid, N., Poulsen, P.C., Elliott, J., Coulson, J., McPhee, J., Robertson, A., da Costa Martins, P.A., Kitmitto, A., Wisløff, U., Cartwright, E.J., Monfredi, O., Lundby, A., Dobrzynski, H., Oceandy, D., Morris, G. M., Boyett, M.R., 2017. Targeting miR-423-5p reverses exercise training-induced HCN4 channel remodeling and sinus bradycardia. Circ. Res. 121, 1058–1068.

Guglielmi, G., Del Re, M., Gol, L.S., Bengala, C., Danesi, R., Fogli, S., 2024. Pharmacological insights on novel oral selective estrogen receptor degraders in breast cancer. Eur. J. Pharmacol. 969, 176424.

Hamilton, E., Oliveira, M., Turner, N., García-Corbacho, J., Hernando, C., Ciruelos, E.M., Kabos, P., Borrego, M.R., Armstrong, A., Patel, M.R., Vaklavas, C., Twelves, C., Boni, V., Incorvati, J., Brier, T., Gibbons, L., Klinowska, T., Lindemann, J.P.O., Morrow, C.J., Sykes, A., Baird, R., 2024a. A phase I dose escalation and expansion trial of the next-generation oral SERD camizestrant in women with ER-positive, HER2-negative advanced breast cancer: SERENA-1 monotherapy results. Ann. Oncol. 35, 707–717.

Hamilton, E.P., Pluard, T.J., Wang, J.S., Morikawa, A., Johnston, S.R.D., Dees, E.C., Vaklavas, C., Armstrong, A.C., Munster, P.N., Unni, N., Wright, G.L.S., Kayali, F., Song, T., Rong, Y., Yamaguchi, K., Juric, D., 2024b. H3B-6545 in women with locally advanced/metastatic estrogen receptor-positive (ER+), HER2 negative (–) breast cancer (BC). J. Clin. Oncol. 42 (16.Suppl), 1015. https://doi.org/10.1200/JCO.2024.42.16_suppl.1015.

Hamilton, E.P., Loibl, S., Bachelot, T., Gnant, M., Niikura, N., Park, Y.H., Tolaney, S.M., Pistilli, B., Rastogi, P., Saini, K.S., Gioni, I., Johnston, S., Nunes, R., Quintana, A., Stuart, M., Syta, E., Walding, A., Klinowska, T., Mayer, I.A., 2025. CAMBRIA-1 & CAMBRIA-2 phase III trials: camizestrant versus standard endocrine therapy in ER+/HER2– early breast cancer. Future Oncol.

Hennis, K., Biel, M., Fenske, S., Wahl-Schott, C., 2022. Paradigm shift: new concepts for HCN4 function in cardiac pacemaking. Pflugers Arch. 474, 649–663.

Jhaveri, K.L., Bellet, M., Turner, N.C., Loi, S., Bardia, A., Boni, V., Sohn, J., Neilan, T.G., Villanueva-Vázquez, R., Kabos, P., García-Estévez, L., López-Miranda, E., Pérez-Fidalgo, J.A., Pérez-García, J.M., Yu, J., Fredrickson, J., Moore, H.M., Chang, C.W., Bond, J.W., Eng-Wong, J., Gates, M.R., Lim, E., 2024. Phase Ia/b study of giredestrant ± palbociclib and ± luteinizing hormone-releasing hormone agonists in estrogen receptor-positive, HER2-negative, locally advanced/metastatic breast cancer. Clin. Cancer Res. 30, 754–766.

Jhaveri, K.L., Neven, P., Casalnuovo, M.L., Kim, S.B., Tokunaga, E., Aftimos, P., Saura, C., O'Shaughnessy, J., Harbeck, N., Carey, L.A., Curigliano, G., Llombart-Cussac, A., Lim, E., Garcia Tinoco, M.L., Sohn, J., Mattar, A., Zhang, Q., Huang, C.S., Hung, C.C., Martinez Rodriguez, J.L., Ruiz Borrego, M., Nakamura, R., Pradhan, K. R., Cramer von Laue, C., Barrett, E., Cao, S., Wang, X.A., Smyth, L.M., Bidard, F.C., Group, E.-S., 2025. Imlunestrant with or without abemaciclib in advanced breast cancer. N. Engl. J. Med. 392, 1189–1202.

Kashou, A.H., Basit, H., Chhabra, L., 2022. Physiology, Sinoatrial Node, StatPearls [Internet]. StatPearls Publishing, Treasure Island, FL.

Lawson, M., Cureton, N., Ros, S., Cheraghchi-Bashi, A., Urosevic, J., D'Arcy, S., Delpuech, O., DuPont, M., Fisher, D.I., Gangl, E.T., Lewis, H., Trueman, D., Wali, N., Williamson, S.C., Moss, J., Montaudon, E., Derrien, H., Marangoni, E., Miragaia, R.J., Gagrica, S., Morentin-Gutierrez, P., Moss, T.A., Maglennon, G., Sutton, D., Polanski, R., Rosen, A., Cairns, J., Zhang, P., Sanchez-Guixe, M., Serra, V., Critchlow, S.E., Scott, J.S., Lindemann, J.P.O., Barry, S.T., Klinowska, T., Morrow, C. J., Carnevalli, L.S., 2023. The next-generation oral selective estrogen receptor degrader camizestrant (AZD9833) suppresses ER+ breast cancer growth and overcomes endocrine and CDK4/6 inhibitor resistance. Cancer Res. 83, 3989–4004.

Long, V., Fiset, C., 2020. Contribution of estrogen to the pregnancy-induced increase in cardiac automaticity. J. Mol. Cell. Cardiol. 147, 27–34.

Montano, N., Cogliati, C., Porta, A., Pagani, M., Malliani, A., Narkiewicz, K., Abboud, F. M., Birkett, C., Somers, V.K., 1998. Central vagotonic effects of atropine modulate spectral oscillations of sympathetic nerve activity. Circulation 98, 1394–1399.

Oliveira, M., Hamilton, E.P., Incorvati, J., Heras, B.B.D.L., Calvo, E., García-Corbacho, J., Ruiz-Borrego, M., Vaklavas, C., Turner, N.C., Ciruelos, E.M., Patel, M.R., Armstrong, A.C., Kabos, P., Twelves, C., Brier, T., Irurzun-Arana, I., Klinowska, T., Lindemann, J.P.O., Morrow, C.J., Baird, R.D., 2022. SERENA-1: updated analyses from a phase 1 study (parts C/D) of the next-generation oral SERD camizestrant (AZD9833) in combination with palbociclib, in women with ER-positive, HER2-negative advanced breast cancer (abstr). J. Clin. Oncol. 40, 1032.

Oliveira, M., Pominchuk, D., Nowecki, Z., Hamilton, E., Kulyaba, Y., Andabekov, T., Hotko, Y., Melkadze, T., Nemsadze, G., Neven, P., Vladimirov, V., Zamagni, C., Denys, H., Forget, F., Horvath, Z., Nesterova, A., Ajimi, M., Kirova, B., Klinowska, T., Lindemann, J.P.O., Lissa, D., Mathewson, A., Morrow, C.J., Traugottova, Z., van Zyl, R., Arkania, E., 2024. Camizestrant, a next-generation oral SERD, versus fulvestrant in post-menopausal women with oestrogen receptor-positive, HER2-negative advanced breast cancer (SERENA-2): a multi-dose, open-label, randomised, phase 2 trial. Lancet Oncol. 25, 1424–1439.

Protze, S.I., Liu, J., Nussinovitch, U., Ohana, L., Backx, P.H., Gepstein, L., Keller, G.M., 2017. Sinoatrial node cardiomyocytes derived from human pluripotent cells function as a biological pacemaker. Nat. Biotechnol. 35, 56–68.

Shi, W., Wymore, R., Yu, H., Wu, J., Wymore, R.T., Pan, Z., Robinson, R.B., Dixon, J.E., McKinnon, D., Cohen, I.S., 1999. Distribution and prevalence of hyperpolarization-activated cation channel (HCN) mRNA expression in cardiac tissues. Circ. Res. 85, e1–e6.

Silva, L.E., Silva, C.A., Salgado, H.C., Fazan Jr., R., 2017. The role of sympathetic and vagal cardiac control on complexity of heart rate dynamics. Am. J. Physiol. Heart Circ. Physiol. 312, H469–H477.

Turner, D., Kang, C., Mesirca, P., Hong, J., Mangoni, M.E., Glukhov, A.V., Sah, R., 2021. Electrophysiological and molecular mechanisms of sinoatrial node mechanosensitivity. Front. Cardiovasc. Med. 8, 662410.

Turner, N., Huang-Bartlett, C., Kalinsky, K., Cristofanilli, M., Bianchini, G., Chia, S., Iwata, H., Janni, W., Ma, C.X., Mayer, E.L., Park, Y.H., Fox, S., Liu, X., McClain, S., Bidard, F.C., 2023a. Design of SERENA-6, a phase III switching trial of camizestrant in ESR1-mutant breast cancer during first-line treatment. Future Oncol. 19, 559–573.

Turner, N., Vaklavas, C., Calvo, E., Garcia-Corbacho, J., Incorvati, J., Borrego, M.R., Twelves, C., Armstrong, A., Bermejo, B., Hamilton, E., Oliveira, M., Ciruelos, E., Kabos, P., Patel, M.R., Borrell, M., Burris, H., de Paula, B., Falcon, A., Hernando, C., Moreno, I., O'Brien, C.S., Shagisultanova, E., Ruiz, I.V., Wang, J.S., Wei, M., Brier, T., Carroll, D., Ciardullo, C., Gibbons, L., Irurzun-Arana, I., Jack, T., Kirova, B., Klinowska, T., Lindemann, J., Maidment, J., Mathewson, A., Maudsley, R., McEwen, R., Morrow, C., Sykes, A., Baird, R.D., 2023b. Abstract P3-07-28: SERENA-1: updated analyses from a phase 1 study of the next generation oral selective estrogen receptor degrader camizestrant (AZD9833) combined with abemaciclib, in women with ER-positive, HER2-negative advanced breast cancer (abstr). Cancer Res. 83. P3-07-28.

Vaklavas, C., Oliveira, M., Armstrong, A., Moreno, I., Twelves, C., Victoria Ruiz, I., Bermejo, B., Ajimi, M., Brier, T., Ciardullo, C., Gibbons, L., Irurzun-Arana, I., Jack, T., Klinowska, T., Lindemann, J., Mathewson, A., Morrow, C., Sykes, A., Baird, R., 2024. Abstract PO3-19-09: SERENA-1: results from a phase 1 study (parts I/J) testing the next-generation oral selective estrogen receptor degrader (SERD) camizestrant (AZD9833) in combination with capivasertib in women with ER+, HER2 advanced breast cancer (abstr). Cancer Res. 84. PO3-19-09.

Zhang, Z., Huang, T.Q., Nepliouev, I., Zhang, H., Barnett, A.S., Rosenberg, P.B., Ou, S.I., Stiber, J.A., 2017. Crizotinib inhibits hyperpolarization-activated cyclic nucleotide-gated channel 4 activity. Cardiooncology 3, 1.